AEROSPACE REPORT NO.
TOR-2013-00430

An Oscillator Model for rf-Discharge Lamps Used in Atomic Clocks: The rf-Discharge as a Complex Permeability Medium

August 15, 2013

James C. Camparo,[1] Fei Wang,[2] Yat Chan,[2] and Warren E. Lybarger[1]
[1]Electronics and Photonics Laboratory
Physical Sciences Laboratories
[2]Communication Systems Implementation Subdivision
Communications and Networking Division

Prepared for:

Space and Missile Systems Center
Air Force Space Command
483 N. Aviation Blvd.
El Segundo, CA 90245-2808

Contract No. FA8802-09-C-0001

Authorized by: Space Systems Group

AEROSPACE
Assuring Space Mission Success

AEROSPACE REPORT NO.
TOR-2013-00430

An Oscillator Model for rf-Discharge Lamps Used in Atomic Clocks: The rf-Discharge as a Complex Permeability Medium

August 15, 2013

James C. Camparo,[1] Fei Wang,[2] Yat Chan,[2] and Warren E. Lybarger[1]
[1]Electronics and Photonics Laboratory
Physical Sciences Laboratories
[2]Communication Systems Implementation Subdivision
Communications and Networking Division

Prepared for:

Space and Missile Systems Center
Air Force Space Command
483 N. Aviation Blvd.
El Segundo, CA 90245-2808

Contract No. FA8802-09-C-0001

Authorized by: Space Systems Group

AEROSPACE
Assuring Space Mission Success

AEROSPACE REPORT NO.
TOR-2013-00430

An Oscillator Model for rf-Discharge Lamps Used in Atomic Clocks: The rf-Discharge as a Complex Permeability Medium

Approved by:

William T. Lotshaw, Director
Photonics Technology Department
Electronics and Photonics Laboratory

Walter F. Buell, Principal Director
Electronics and Photonics Laboratory
Physical Sciences Laboratories

Diana M. Johnson, Principal Director
Communication Systems
Implementation Subdivision
Communications and Networking Division

Eileen Z. Wang, Systems Director
GPS III Nav Payload
Navigation Division
Space Systems Group

SC-2296(5630, 6, JS)

Contents

Figures

An Oscillator Model for rf-Discharge Lamps Used in Atomic Clocks: The rf-Discharge as a Complex Permeability Medium

J. Camparo,[1] F. Wang,[2] Y. Chan,[2] and W. Lybarger[1]

[1]*Physical Sciences Laboratories*
and
[2]*Communications Networking Division*
The Aerospace Corporation, 2310 E. El Segundo Blvd., El Segundo, CA

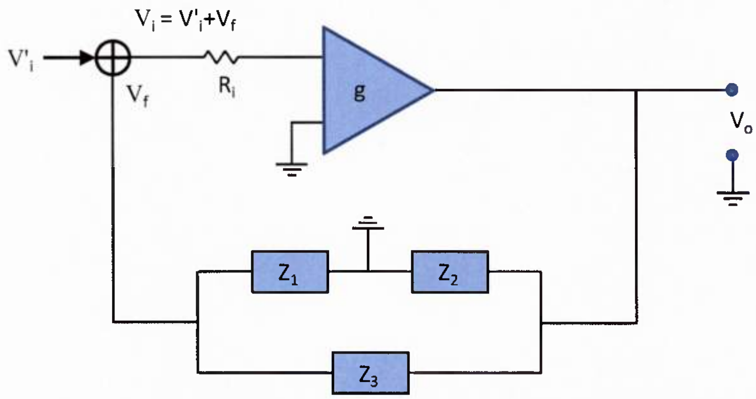

Figure 1: A feedback model for the Colpitts or Hartley oscillator used to drive rf-discharge lamps in vapor-cell atomic clocks. For the Colpitts oscillator, Z_2 and Z_3 are capacitors with Z_1 an inductor. For the Hartley oscillator, Z_2 and Z_3 are inductors with Z_1 a capacitor. In either case, an inductor is assumed to surround the glass bulb of the rf-discharge lamp, thereby providing energy to ionize the Rb atoms and generate resonant light.

Abstract

In the rf-discharge lamp of an atomic clock, the inductor of a Colpitts or Hartley oscillator surrounds a glass bulb containing a vapor of Rb and a noble gas (typically Xe or Kr). Rf-energy is extracted from the field leading to ionization of the Rb, and in recombination with electrons these Rb ions produce the resonant light necessary for atomic signal generation. From an electrical perspective, the discharge can be viewed as a permeable medium located inside an inductor's coils. This permeable medium, however, must have both a real and an imaginary part: not only does the discharge alter the phase of the circuit's rf-field, it also extracts energy from the resonant circuit. Here, we consider the manner in which this complex permeability enters the electrical description of the oscillator, and its likely dependence on discharge parameters.

I. Introduction

We consider the very general oscillator feedback circuit illustrated in Fig. 1, where an external AC voltage V'_i is added to a feedback signal, V_f, to produce the input voltage V_i for an amplifier. Of course, the key element in the figure is the network of complex impedances in the feedback loop, which typically take one of two configurations [1]: a Colpitts oscillator configuration, where Z_2 and Z_3 are capacitors with Z_1 the loop-inductor surrounding a lamp's glass bulb; or a Hartley oscillator, where Z_1 is a capacitor, and Z_2 and Z_3 are inductors (one of which corresponds to the wire loops surrounding a lamps' glass bulb [2,3]).

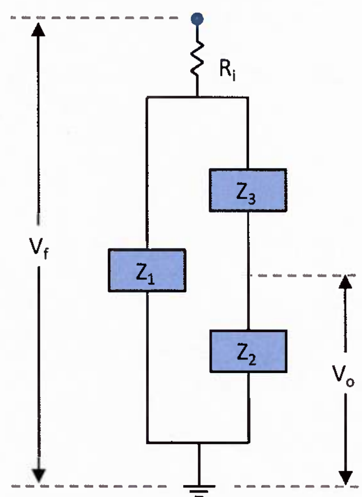

Figure 2: Figure 1 redrawn. Here, V_f is the input voltage to the amplifier.

Focusing for the moment on the feedback portion of Fig.1, this can be redrawn as Fig. 2, and from this figure it is straightforward to show that

$$V_o = \frac{V_f Z_1 Z_2}{R_i(Z_1+Z_2+Z_3)+Z_1(Z_2+Z_3)} \equiv \frac{V_f}{\kappa}. \quad (1)$$

Then, returning to Fig. 1, we see that

$$V_o = gV_i = g(V_i' + V_f), \quad (2a)$$

and from Eq. (1) this yields

$$V_o = \frac{gV_i'}{1-g\kappa}. \quad (2b)$$

The only way V_o can be non-zero without an input signal V'_i (i.e., the only way the circuit can self-oscillate) is if $g\kappa = 1$. Since g is real, self-oscillation implies that κ must also be real. In other words, the feedback signal must return to the amplifier input in phase (i.e., with $V_f = |V_f|e^{i\theta}$, θ must equal $2n\pi$ where n is an integer). Thus, for self-oscillation we require that

$$\mathrm{Re}[\kappa] = \frac{1}{g} \quad \text{and} \quad \mathrm{Im}[\kappa] = 0. \quad (3)$$

If, to first order, we assume that the Z_i are pure inductors and capacitors, then from Eq. (1) it is clear that

$$\mathrm{Im}[\kappa] = Z_1 + Z_2 + Z_3 = 0. \quad (4a)$$

$$\mathrm{Re}[\kappa] = \frac{Z_2+Z_3}{Z_2} \Rightarrow -\frac{Z_2}{Z_1} = g. \quad (4b)$$

Thus, in order for g to be positive, we see from Eq. (4b) that oscillation limits the choices for the Z_i: if Z_1 is an inductor then Z_2 must be a capacitor; alternatively, if Z_1 is a capacitor than Z_2 must be an inductor.

II. The Inductor in a Real Discharge Lamp

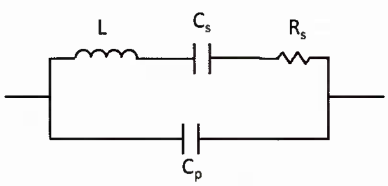

Figure 3: In a real rf-discharge lamp, the impedance Z_i that corresponds to the loops of wire surrounding the lamp's glass bulb should be replaced with the RLC circuit shown here. For the Colpitts lamp oscillator that we used in our experiments (i.e., L = 650 nH), one of us (FW) measured C_s = 3.7 pF, R_s = 8 Ω, and C_p = 9 pF.

Recent measurements made by one of us (FW) clearly demonstrate that in a real rf-discharge lamp oscillator there is a subtlety that must be included in the model of Section I. Briefly, whatever element in the feedback network corresponds to the loop inductor surrounding the lamp's glass bulb, we must consider this as a resonant RLC circuit as illustrated in Fig. 3. Briefly, C_s and R_s are the series capacitance and resistance, respectively, which must exist for real loops of wire; while the parallel capacitor, C_p, represents the capacitance that must exist between the loops of wire and the lamp's metal housing.

Defining Z_L as the complex impedance of the RLC circuit, it is straightforward to show that in the absence of a discharge (i.e., the inductor loops simply surround air) that

$$\mathrm{Re}[Z_L] = \frac{(f-1)C_s R_s}{\omega^2 C_p C_s^2 R_s^2 + f^2 C_p\left(\frac{\omega^2}{\omega_L^2}-1\right)^2} \quad (5a)$$

$$\mathrm{Im}[Z_L] = \frac{f\left(\frac{\omega^2}{\omega_L^2}f-1\right)\left(1-\frac{\omega^2}{\omega_L^2}\right)-\omega^2 C_s^2 R_s^2}{\omega^3 C_p C_s^2 R_s^2 + \omega f^2 C_p\left(\frac{\omega^2}{\omega_L^2}-1\right)^2}. \quad (5b)$$

In these expressions,

$$\omega_L \equiv \sqrt{\frac{C_s+C_p}{LC_sC_p}} \quad \text{and} \quad f \equiv \frac{C_s+C_p}{C_p} \quad (6)$$

Figure 4 shows plots of $\mathrm{Re}[Z_L]$ and $\mathrm{Im}[Z_L]$ as functions of frequency for the parameters that were measured for our experimental setup, and which are given in the caption of Fig. 3.

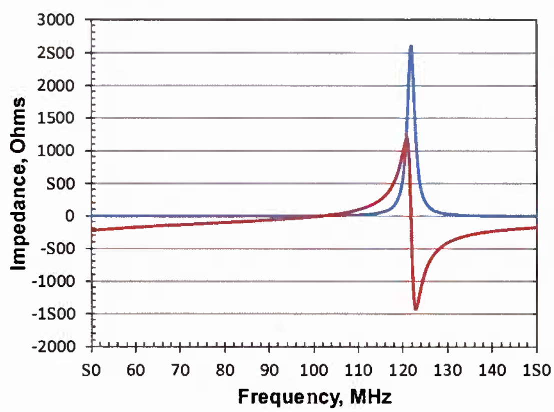

Figure 4: Real (blue) and imaginary (red) parts of the complex impedance for the RLC model of the inductor loops that surround the lamp's glass bulb (assuming no discharge). We employed the parameters given in the caption of Fig. 3.

As illustrated in Fig. 5, to include the influence of the discharge in Eqs. (5), we let $L \rightarrow \mu L$, where μ is a complex scalar permeability: $\mu = \alpha - i\beta$ [4]. Here, α describes that part of the plasma discharge that gives

rise to a phase shift of the rf-field, and which we expect will influence the resonant frequency of the RLC circuit, ω_L. β describes rf-energy extraction by the discharge, and so we expect it to contribute to R_s.

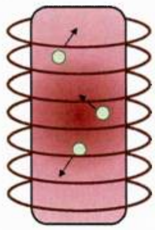

Figure 5: In the rf-discharge lamp of an atomic clock, the inductor coils of the Colpitts or Hartley oscillator surround a glass bulb that contains Rb and a noble gas (e.g., Xe or Kr). Since rf-energy is extracted from the field to ionize the Rb, the permeability of the material inside the inductor must have an imaginary part that leads to resistance.

Without going into all the details here, an analysis of Fig. 3 including a term for the discharge's permeability gives credence to these expectations. Thus, in order to include the discharge in Eqs. (5) and (6) we need only make the replacements

$$\omega_L \rightarrow \frac{\omega_L}{\sqrt{\alpha}} = \sqrt{\frac{C_s + C_p}{\alpha L C_s C_p}} \tag{7a}$$

and

$$R_s \rightarrow R_s + \left(\frac{\beta}{\alpha}\right)\frac{\omega f}{\omega_L^2 C_s}. \tag{7b}$$

Figure 6 shows plots of $\mathrm{Re}[Z_L]$ and $\mathrm{Im}[Z_L]$ with a discharge present: $\alpha = 1.2$ and $\beta/\alpha = 0.01$. Figure 7 is similar, but with $\beta/\alpha = 0.03$.

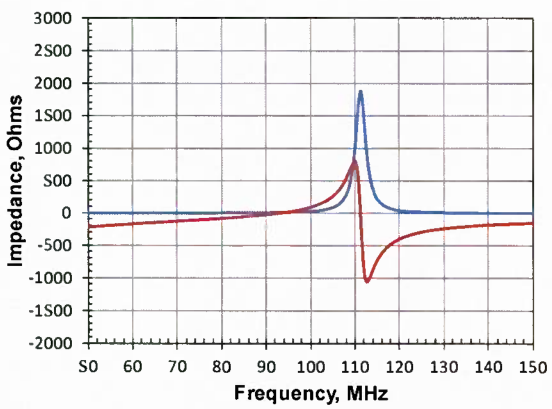

Figure 6: Real (blue) and imaginary (red) parts of the complex impedance for the RLC model of Fig. 3 with $\alpha = 1.2$ and $\beta/\alpha = 0.01$.

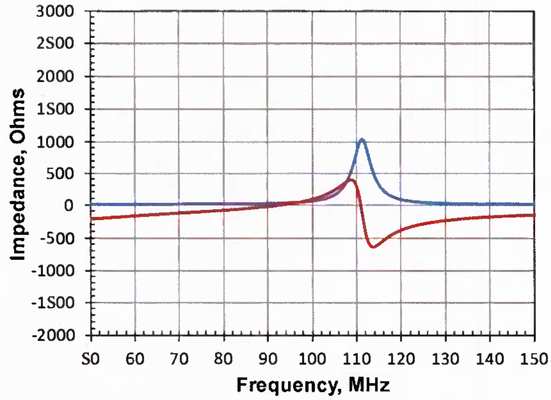

Figure 7: Real (blue) and imaginary (red) parts of the complex impedance for the RLC model of Fig. 3 with $\alpha = 1.2$ and $\beta/\alpha = 0.03$.

As illustrated in Figs. 5, 6, and 7, $\mathrm{Im}[Z_L]$ crosses zero at two locations near ω_L. From Eq. (5b), it is straightforward to calculate these zero crossings in the case that $\omega C_s R_s << 1$, which will typically be the case (even when the discharge is present). We define ω_s as the series resonant frequency and ω_p as the parallel resonant frequency:

$$\omega_s, \omega_p = \frac{\omega_L}{\sqrt{2}}\sqrt{1 + f^{-1} \pm f^{-1}\sqrt{f^2 - 2f + 1}}\ , \tag{8}$$

Here, the plus and minus signs refer to ω_s and ω_p, respectively, and we note from Eq. (6) that $f \geq 1$. Typically, the oscillator will resonate at ω_s, since it is at this frequency that the real part of the impedance is minimized.

III. The Colpitts Oscillator

As a consequence of the considerations presented in Section II, and referring to Fig. 2, for a Colpitts oscillator we take

$$Z_2 = R_C - \frac{i}{\omega C_2}, \quad Z_3 = R_C - \frac{i}{\omega C_3}, \tag{9a}$$

$$Z_1 = \mathrm{Re}[Z_L] + i\mathrm{Im}[Z_L]. \tag{9b}$$

Here, R_C is the equivalent series resistance that we expect for a real capacitor, but which we will henceforth assume is zero.

To determine the resonant frequency of the Colpitts oscillator we employ Eq. (4a) along with Eqs. (5), (7) and (8). First, however, we note that in Colpitts oscillator circuit used in our experiments we have $C_3 = 150$ pF and $C_2 = 30$ pF. Thus, if we define a "Colpitts capacitance," C_{CP}, as

$$C_{CP} = \frac{C_2 C_3}{C_2 + C_3}, \qquad (10)$$

then in our case we have C_{CP} = 25 pF, so that C_p/C_{CP} = 0.36 and $C_s/C_{CP} \cong 0.15$. Thus, while the Colpitts capacitance is greater than the capacitances occurring in the RLC circuit of the lamp's coils, it is not significantly greater. Consequently, the complex impedance of these capacitors cannot be ignored, and we have from Eq. (4a)

$$\mathrm{Im}[Z_L] - \frac{1}{\omega C_2} - \frac{1}{\omega C_3} = 0 =$$

$$\frac{f\left(\frac{\omega^2}{\omega_L^2} f - 1\right)\left(1 - \frac{\omega^2}{\omega_L^2}\right) - \omega^2 C_s^2 R_s^2}{\omega^3 C_p C_s^2 R_s^2 + \omega f^2 C_p \left(\frac{\omega^2}{\omega_L^2} - 1\right)^2} - \frac{1}{\omega C_{CP}}. \qquad (11)$$

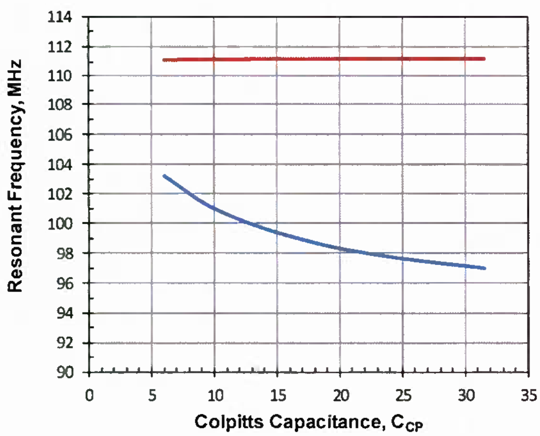

Figure 8: The parallel resonant frequency (red), ω_p, and series resonant frequency (blue), ω_s, of the Colpitts oscillator.

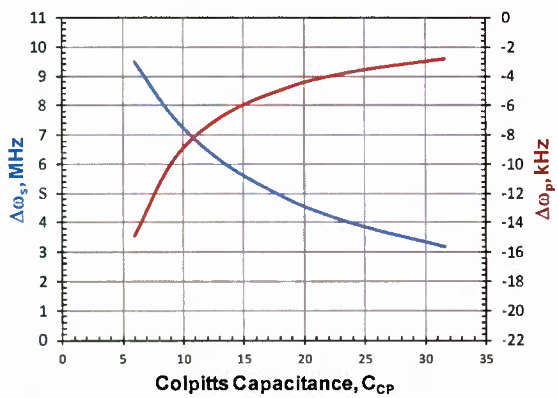

Figure 9: The difference between the parallel resonant frequency (red) and the series resonant frequency (blue) from their values in the case of $C_{CP} \to \infty$. Notice that the units for the parallel resonant frequency difference are kilohertz.

Solving Eq. (11) numerically for the series and parallel resonant frequencies, ω_s and ω_p, respectively, Figs. 8 and 9 show ω_s and ω_p as functions of C_{CP} with α = 1.2 and β/α = 0.01. Figure 8 shows the actual resonant frequencies, while Fig. 9 shows the difference between these frequencies and the resonant frequencies in the case that $C_{CP} \to \infty$. (Notice in Fig. 9 that the units for $\Delta\omega_p$ are kHz.) Clearly, the Colpitts capacitance has a small but non-negligible effect on ω_s, affecting its value by ~ 4 % in our case of C_{CP} = 25 pF. Alternatively, the Colpitts capacitance has hardly any effect on ω_p, affecting its value by ~ 0.016 % in our case. Thus, while the Colpitts capacitors C_2 and C_3 cannot be ignored, the resonant frequency of the oscillator is primarily determined by the RLC circuit of the lamp coils illustrated in Fig. 3. This will most certainly vary from lamp to lamp (even for the same circuit design), and likely gives rise to some of the variability among Rb clock lamp oscillators.

IV. Physical Model for β

In this section, we attempt to tie β to physical characteristics of the discharge. To begin, we first note that as a resistance term, we expect β to be proportional to the circuit's power loss. More specifically, we expect β to represent electrical power that flows *out* of the circuit, *into* the discharge, and from the discharge is *irreversibly lost*.

Without too much difficulty, we can imagine at least three processes that lead to irreversible energy flow out of the discharge: discharge heating of the bulb's glass walls [5,6], electron excitation of Xe and the resulting Xe photon emission [7], and electron/Rb^+ recombination leading to photon emission [7]. We do not include Rb ionization in this list, since ionization by itself does not represent energy loss; energy is only lost by the discharge when those ions recombine with electrons and emit a photon that *escapes the discharge*. In this regard, it is important to note that radiation trapping [8,9] likely limits the discharge's energy loss by electron/Rb^+ recombination, since the energy carried by the radiation-trapped photon has a high probability of getting back into the discharge.

We therefore write

$$\beta \sim \gamma_{TH}(T - T_{DC}) + \frac{\gamma_{Xe}}{(kT_e)^{3/2}} \int_{\varepsilon_1}^{\infty} \sqrt{x}\, e^{-x/kT_e} dx + \left(\gamma_D n^2 - \Gamma_{RT}([Rb])\right). \qquad (12)$$

The first term on the right-hand-side of Eq. (12) represents rf-heating: T_{DC} is the temperature of the

discharge when the rf-field supplies *no* additional heat (i.e., it is the temperature of the discharge as defined by a DC heater around the lamp bulb) and $1/\gamma_{TH}$ is a thermal time constant. The second term on the right-hand-side of Eq. (12) corresponds to electron excitation of Xe: ε_1 is the first excited state of Xe at 8.4 eV, and T_e is the electron temperature. From our lamp's spectra we estimate $T_e \sim 3500$ K [5], so that $kT_e \sim 0.3$ eV. Finally, the last term in brackets on the right-hand-side of Eq. (12) represents electron/Rb^+ recombination. Since we expect charge neutrality in the discharge, the density of Rb^+ should equal the density of free electrons, and the rate of recombination should be proportional to those two densities multiplied by an ambipolar diffusion time constant, $1/\gamma_D$. Further, we reduce the loss of electron/Rb^+ recombination by a radiation-trapping term, Γ_{RT}, which we expect will be some complicated function of the neutral rubidium atom density in the discharge, [Rb].

Focusing on the Xe excitation term, we write

$$\beta_{Xe} \equiv \frac{\gamma_{Xe}}{(kT_e)^{3/2}} \int_{\varepsilon_1}^{\infty} \sqrt{x}\, e^{-x/kT_e} dx \cdot \qquad (13)$$

Then, evaluating the integral we get

$$\frac{\beta_{Xe}}{\gamma_{Xe}} = \sqrt{\frac{\varepsilon_1}{kT_e}}\, e^{-\varepsilon_1/kT_e} + \frac{\sqrt{\pi}}{2} \mathrm{Erfc}\left[\sqrt{\frac{\varepsilon_1}{kT_e}}\right], \qquad (14)$$

where Erfc[...] is the complimentary error function [10]. Note, however, that $\varepsilon_1/kT_e \sim 28$, so that the first term on the right-hand-side of Eq. (14) has a value of $\sim 4\times10^{-12}$, while the second term on the right-hand-side of Eq. (14) has a value of $\sim 6\times10^{-14}$. Thus, to good approximation for our limited range of T_e values we can ignore the second term on the right-hand-side of Eq. (14) and write

$$\beta_{Xe} \cong \gamma_{Xe} \sqrt{\frac{\varepsilon_1}{kT_e}}\, e^{-\varepsilon_1/kT_e} . \qquad (15)$$

Figure 10 shows $\Delta\beta/\Delta\beta_{max}$ and $\Delta\beta_{Xe}/\Delta\beta_{Xe,max}$ as functions of lamp temperature from our measurements of a Colpitts-oscillator lamp. Briefly, we measure the complex impedance of the lamp coils illustrated in Fig. 3 at the oscillation frequency, and from that measurement determine α and β. Here, we define $\Delta\beta/\Delta\beta_{max}$ as

$$\frac{\Delta\beta}{\Delta\beta_{max}} \equiv \frac{\beta - \beta_{min}}{\beta_{max} - \beta_{min}}, \qquad (16)$$

with a similar expression for $\Delta\beta_{Xe}/\Delta\beta_{Xe,max}$. The fact that $\Delta\beta/\Delta\beta_{max}$ and $\Delta\beta_{Xe}/\Delta\beta_{Xe,max}$ track each other so well suggests that our physical model for β has value. Additionally, it suggests that at low lamp temperatures (i.e., T ≤ 138 °C) changes in β derive principally from changes in electron temperature. Though we don't as yet have a good understanding of why β increases at high temperatures (i.e., T > 138 °C), it may be that the electron density in the discharge increases at these higher temperatures, or that radiation-trapping is less efficient at returning the energy of electron/Rb^+ recombination photons to the discharge (and hence the electrical circuit).

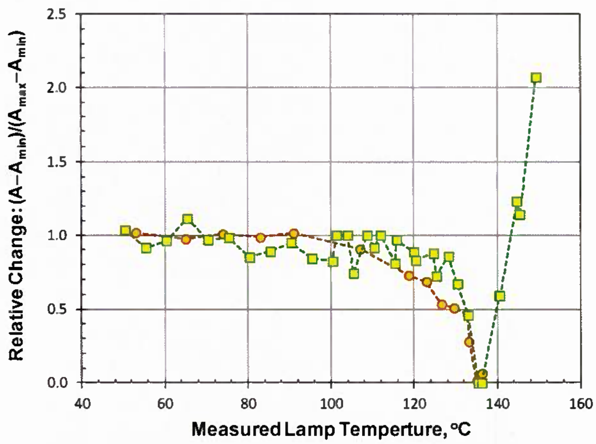

Figure 10: $\Delta\beta/\Delta\beta_{max}$ (yellow squares) and $\Delta\beta_{Xe}/\Delta\beta_{Xe,max}$ (orange circles) as a function of lamp temperature for our lamp operating at nominal rf-power.

V. Summary

In analyzing an atomic clock's rf-discharge lamp oscillator, we found that the lamp coils must be modeled as an RLC circuit if the electrical characteristics of the oscillator are to be properly understood. Further, from an electrical perspective, the plasma inside the lamp cannot be ignored, and that this should be included in the circuit analysis as a permeable medium with a real and an imaginary part: $\mu = \alpha - i\beta$. Re[μ] plays a primary role in determining the lamp circuit's resonant frequency, while Im[μ] plays an important role in determining the circuit's energy loss (i.e., the circuit's Q). Finally, we considered the discharge processes that likely contribute to Im[μ], and presented evidence for a primary played by electron temperature.

References

1. J. D. Ryder, Electronic Fundamentals and Applications (Prentice Hall, Englewood Cliffs, NJ, 1970), Ch. 15.

2. R. G. Brewer, "High intensity low noise rubidium light source," Rev. Sci. Instrum. 32(12), 1356 (1961).

3. B. Budick, R. Novick, and A. Lurio, "Light sources for double resonance level crossing spectroscopy," Appl. Opt. 4(2), 229 (1965).

4. A. Von Hippel, Dielectrics and Waves (Wiley, New York, 1954).

5. J. Coffer and J. Camparo, "rf-power and the ring-mode to red-mode transition in an inductively coupled plasma," J. Appl. Phys. 111, 083304 (2012).

6. J. Coffer, M. Huang, and J. Camparo "Self-pulsing in alkali rf-discharge lamps," Proceedings 2012 IEEE International Frequency Control Symposium (IEEE Press, Piscataway, NJ, 2012) pp. 692-696.

7. J. Camparo and R. Mackay, "Spectral mode changes in an alkali rf discharge," J. Appl. Phys. 101, 053303 (2007).

8. R. Cowan and G. Dieke, "Self-absorption of spectrum lines," Rev. Mod. Phys. 20(2), 418-455 (1948).

9. M. Chevrollier, "Radiation trapping and Lévy flights in atomic vapours: an introductory review," Contemp. Phys. 53(3), 227-239 (2012).

10. M. Abramowitz and I. A. Stegun, Handbook of Mathematical Functions with Formulas, Graphs, and Mathematical Tables, (National Bureau of Standards, Applied Mathematics Series 55, 1964).

Equipment Calibration Information

Technical Reports Addendum Asset Summary

AEROSPACE

TRAAS ID #: 2013062710014129041

Report Name: An Oscillator Model for rf-Discharge Lamps Used in Atomic Clocks: The rf-Discharge as a Complex Permeability Medium

Aerospace Report Number: TOR-2013-00430

Start Date of Test: 2012-08-27 Created By: 29041 Wang, Fei JO: 159026

End Date of Test: 2012-11-19 First Aerospace Author / PI: 16259 Camparo, James C

Program: GPSIII

Description:

Keywords:

Asset: AAH678 Manufacturer: TEKTRONIX INCORPORATED Model: TDS5054 Usage Start Date: 2012-08-27 Usage End Date: 2012-11-19 Asset Comment:

Date:	Calibration Due Date:	Comment:	Certificate Number:
2012-08-06	2012-10-14	Extension	a988422af11c184897d82d74d9f8fa2d

Asset: ACR873 Manufacturer: OCEAN OPTICS Model: HR4000CG-UV-NIR Usage Start Date: 2012-08-27 Usage End Date: 2012-11-19 Asset Comment:

Date:	Calibration Due Date	Comment:	Certificate Number:
2012-01-26	2013-01-20	TMT-NORMAL	319f394413b84548871c6ec7b06a0a83

Asset: ACW375 Manufacturer: ANALOGIC CORPORATION Model: MEASUROMETER II Usage Start Date: 2012-08-27 Usage End Date: 2012-11-19 Asset Comment: ACW375 was sent in for calibration after measurement was finished, and it was determined to be within tolerance without any adjustments. The calibration results are as follows: "For the Ice slush test your Analogic thermometer read 0.1 deg C. For the boiling water test your thermometer read between 100.1 and 100.2 deg C. All other tests used resistors and bypassed your RTD."

Date	Calibration Due Date	Comment	Certificate Number
		No Calibration Data Available	

Asset: CC904 Manufacturer: HEWLETT PACKARD CORP. Model: 8592B Usage Start Date: 2012-08-27 Usage End Date: 2012-11-19 Asset Comment:

Date	Calibration Due Date	Comment	Certificate Number
2012-03-07	2012-06-03	Extension	15e686bb268153489a8aa5138c8a8a61
2012-10-15	2013-05-12	TMT-NORMAL	088464152a9baf4bb3971758bed353ee

*Support and Auxillary Equipment are not calibrated.

The Aerospace Corporation
2310 E. El Segundo Boulevard
El Segundo, California 90245-4609
U.S.A.